one in four of the surface Ga atoms is missing and that the remaining surface atoms undergo an inward relaxation. Total energy calculations [48.2] have shown that a relaxed, vacancy surface is energetically favorable for GaAs(111)(2×2) but unfavorable for GaAs($\bar{1}\bar{1}\bar{1}$)(2×2).

Surface band-structure calculations have been carried out by *Nishida* [48.8] for (1×1) GaAs(111) and GaAs($\bar{1}\bar{1}\bar{1}$) surfaces with uniformly contracted [GaAs(111)] and expanded [GaAs($\bar{1}\bar{1}\bar{1}$)] surface atomic layers. *Nishida* found the p_z-like dangling bond band to be very close to the edge of the projected bulk bands for expanded GaAs($\bar{1}\bar{1}\bar{1}$) and significantly above the bulk valence band for relaxed GaAs(111). The uppermost occupied surface band in the latter case was a p_x band which was degenerate with the projected bulk bands. These findings are qualitatively consistent with the polarization dependence of our (2×2) data. The uppermost occupied surface states near the zone boundary showed an increase (decrease) in relative intensity as the polarization vector moved towards the surface normal for GaAs($\bar{1}\bar{1}\bar{1}$)(2×2) [GaAs(111)(2×2)].

In conclusion, the data in Figs.48.2-4 make it clear that the electronic structure of the two surfaces is remarkably different. The origin of the difference must lie in either a different surface geometry or in the effect of interchanging Ga and As atoms. It is likely that both of these are important. There is evidence that the depth of the reconstruction or the degree of bond alteration is greater in the ($\bar{1}\bar{1}\bar{1}$) case. It can be seen in Fig. 48.3 that the agreement between the bulk calculation and the data is much closer for the (111) surface, allowing a clearer separation between bulk and surface features in the spectra. The fact that the strong surface features in GaAs(111) have an apparent (1×1) repeat whereas the (2×2) symmetry is seen clearly for GaAs($\bar{1}\bar{1}\bar{1}$) may indicate that the (2×2) potential is weaker in the (111) case. Although the true dispersion is (2×2), the non-(1×1) dispersion may be too weak to be seen, especially when degenerate with the bulk bands.

Acknowledgments. We are grateful for useful discussions with D.J. Chadi and J. Northrup and for the skillful assistance of B.K. Krusor and L.E. Swartz. Part of this work was supported by NSF Grant DMR 81-08343, and was performed at SSRL which is supported by the Department of Energy, Office of Basic Energy Sciences; and the National Science Foundation, Division of Materials Research.

References

48.1 S.Y. Tong, G. Xu, W.N. Mei: Phys. Rev. Lett. **52**, 1693 (1984) and this Volume, p.303
48.2 D.J. Chadi: Phys. Rev. Lett. **52**, 1911 (1984)
48.3 R.D. Bringans, R.Z. Bachrach: Proc. Int. Soc. Opt. Engineering **447**, 58 (1983)
48.4 R.D. Bringans, R.Z. Bachrach: Proc. 17th Int. Conf. Phys. Semiconductors (to be published)
48.5 D. Haneman: Phys. Rev. **121**, 1063 (1961)
48.6 K. Jakobi, C. von Muschwitz, W. Ranke: Surf. Sci. **82**, 270 (1979)
48.7 W.A. Harrison: J. Vac. Sci. Technol. **16**, 1492 (1979)
48.8 M. Nishida: J. Phys. C**14**, 535 (1981)

49. X-Ray Diffraction from the (3×3) Reconstructed ($\bar{1}\bar{1}\bar{1}$)B Surface of InSb

R.L. Johnson and J.H. Fock

Max-Planck-Institut für Festkörperforschung
Heisenbergstr. 1, D-7000 Stuttgart 80, FRG

I.K. Robinson
AT & T Bell Laboratories, Murray Hill, New Jersey 07974, USA

J. Bohr, R. Feidenhans'l, J. Als-Nielsen, M. Nielsen, and M. Toney
Risø National Laboratory, Risø, DK-4000 Roskilde, Denmark

X-ray diffraction measurements have been performed with synchrotron radiation under UHV conditions on the Sb rich ($\bar{1}\bar{1}\bar{1}$) surface of InSb. This InSb ($\bar{1}\bar{1}\bar{1}$) B surface has a (3×3) reconstruction [49.1]. The surface was prepared by argon-ion bombardment and annealing at 400°C and was characterized using LEED and high-resolution photoemission. Using X-rays incident at the critical angle for total reflection (0.31°) we have measured the intensities of fractional-order Bragg rods corresponding to the (3×3) reconstruction on the B surface.

49.1 Introduction

Standard X-ray crystallographic techniques can be applied to the study of surfaces. In general, scattering from the bulk of the crystal will mask the much weaker signal originating from the surface. If the X-rays are incident at the critical angle for total reflection, then the surface contribution is enhanced [49.2]. *Marra* et al. [49.3] were the first to exploit this technique to study Al-GaAs interfaces using a rotating anode source. They subsequently studied the Ge(001)-(2×1) surface [49.4] using both the rotating anode and synchrotron radiation (SR) and obtained two orders of magnitude more intensity with SR. This technique has the sensitivity and simplicity of interpretation necessary to perform crystallography on reconstructed surfaces and adsorbed monolayers.

At HASYLAB (Hamburger Synchrotronstrahlungslabor, DESY) on adjacent beamlines we have a high precision X-ray diffractometer and a high-resolution angle-resolved photoemission system (20-200 eV) with extensive sample preparation and multiple-technique analysis capabilities. By use of a transfer cell (Fig.49.1) we can take full advantage of both facilities. The sample is prepared and characterized using LEED and photoemission. It is then transferred under UHV conditions (typically 2×10^{-10}mbar) to a small cell fitted with a 0.5 mm thick cylindrical Be window which allows 360° access to X-rays. Valves on the transfer cell and on the photoemission system allow samples to be transferred back and forth easily. After removing the transfer cell from the photoemission system, it is mounted on the goniometer head of the diffractometer for the X-ray measurements.

We chose to study InSb as a prototype zinc-blende structure III-V compound semiconductor with structural properties similar to GaAs. The heavy atoms have large scattering amplitudes, which enable more accurate structure determinations. The InSb($\bar{1}\bar{1}\bar{1}$)B surface (Sb rich) has a (3×3) surface

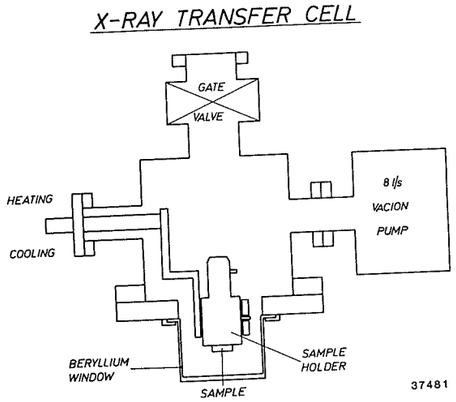

Fig.49.1. Schema of the X-ray transfer cell. The beryllium window allows 360° access for X-rays to the sample surface. The total weight of the cell is about 15 kg

reconstruction, whereas the InSb(111)A surface (In rich) has a (2×2) reconstruction [49.1]. High-quality crystals were available from the Max Planck Institut in Stuttgart.

49.2 Experimental

Accurately oriented, cut and polished samples were cleaned by repeated cycles of sputtering with 500 eV Ar^+ ions and annealing at ~400°C. Valence band energy distribution curves (EDCs) were recorded at $\hbar\omega = 30$ eV to determine surface cleanliness. The quality of the surface reconstruction was checked by observing LEED patterns at different points on the surface. It was found that the valence band EDCs were much more sensitive to contamination than either XPS or LEED measurements. Once a sample was clean and exhibited a reconstruction with sharp fractional order LEED spots, it was transferred to the X-ray cell and mounted on the goniometer. The pressure in the cell was monitored using the the ion-pump current and was below 1×10^{-9} mbar at all times.

The geometry used in our X-ray diffraction experiments is shown in Fig. 49.2. The nature of SR provides good (~0.005°) collimation in the vertical direction. The monochromator arrangement, set for $\lambda = 1.5$ Å, gave a similar collimation in the horizontal direction. Thus, we can choose to place the diffraction plane horizontal and achieve high resolution in both definition of incidence angle and in-plane diffraction. The position of the total reflected beam was used to check the horizontal alignment of the sample optical surface as it was rotated through 360°.

The X-ray intensities were measured with a position-sensitive detector, placed horizontally to resolve a 4° range of scattering angles simultaneously. Data were collected for 50 fractional-order in-plane surface reflections. The maximum count rate was ~180 c/min obtained at the (1/3,0) surface reflection. For several reflections the intensity along the rod was measured to check the two-dimensional character. Symmetry equivalents were used to

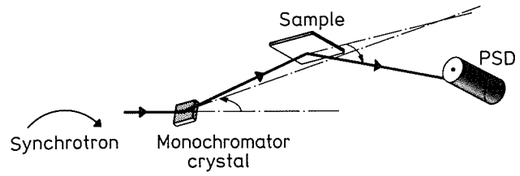

Fig.49.2. Schema of the experimental setup. The white synchrotron radiation is monochromatized by a vertical Ge(111) crystal. The sample surface is precisely horizontal and the grazing angle of incidence is controlled by tilting the monochromator. The position-sensitive detector (PSD) lies in the horizontal scattering plane. Harmonics are filtered away by a flat, gold-plated glass mirror in front of the monochromator

derive intensity error bars. The intensities were also monitored as a function of time to correct for deterioration of the surface.

49.3 Analysis

The structure factor amplitudes $|F_G|$ derived from measured intensities were applied to a calculation of the Patterson function [49.5] (Fig.49.3a),

$$P(\mathbf{R}) = \sum_{\mathbf{G}} |F_G|^2 \cos(\mathbf{R} \cdot \mathbf{G}) \quad ,$$

where $\mathbf{G}$ are the reciprocal lattice vectors, and $\mathbf{R}$ is the position in the surface plane. Interpreting $P(\mathbf{R})$ as the pair correlation of the atomic positions, we find strong peaks (I and II in Fig.49.3a) for interatomic vectors somewhat shorter than in the bulk, one parallel to the unit cell edge and the other at about 30° to it. A rearrangement of a layer of nine

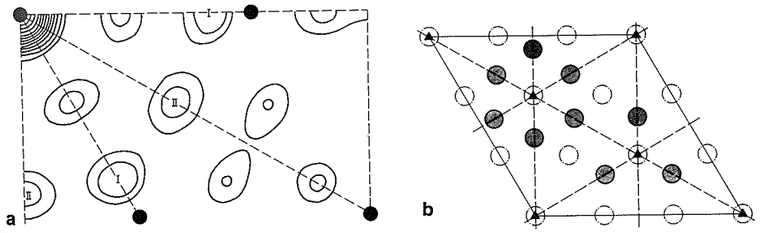

Fig.49.3. (**a**) Contour plot of the Patterson function $P(\mathbf{R})$. Positive, equally spaced contours are shown. Mirror lines in the 2D map are indicated by dashed lines. As a guide to the scale, dots mark lattice vectors of a bulk InSb unit cell. (**b**) Preliminary model of the atomic arrangement in the InSb $(\bar{1}\bar{1}\bar{1})$B (3×3) reconstructed surface. We were unable to distinguish between In and Sb atoms. Nine atoms (shaded circles), constrained by the 3m symmetry shown, have three in-plane positional parameters that have been refined. For reference, an unreconstructed second layer of atoms (broken open circles) is shown. The model is the best one obtained so far, but is only partially in agreement with the data

surface atoms in the 3 × 3 unit cell that is consistent with this and explains the remaining peaks in the Patterson function is shown in Fig.49.3b. Least-squares refinement of these atomic positions subject to the 3m mirror and 3-fold symmetry imposed, agreed only at the two-standard-deviation level. It is likely that a model with a different number of atoms and/or displacements in the second layer is needed to account for the discrepancy. Work is presently in progress to improve the quantity and quality of the data and to investigate other models.

References

49.1 J.T. Grant, T.W. Hass: J. Vac. Sci. Tech. **8**, 94 (1971)
49.2 G.H. Vineyard: Phys. Rev. B**26**, 4146 (1982)
49.3 W.C. Marra, P. Eisenberger, A.Y. Cho: J. Appl. Phys. **50**, 6927 (1979)
49.4 P. Eisenberger, W.C. Marra: Phys. Rev. Lett. **46**, 1081 (1981)
49.5 I.K. Robinson: Phys. Rev. Lett. **50**, 1145 (1983);
B.E. Warren: X-ray Diffraction (Addison-Wesley, Reading, MA 1969)